NANO LETTERS

2007
Vol. 7, No. 4
1086−1090

Broadband Electrical Characterization of Multiwalled Carbon Nanotubes and Contacts

Paul Rice*

Materials Reliability Division, National Institute of Standards and Technology, Boulder, Colorado 80305, and Department of Mechanical Engineering, University of Colorado, Boulder, Colorado 80309

T. Mitch Wallis, Stephen E. Russek, and Pavel Kabos

Electromagnetics Division, National Institute of Standards and Technology, Boulder, Colorado 80305

Received November 21, 2006; Revised Manuscript Received February 13, 2007

ABSTRACT

The electrical response of an individual multiwalled carbon nanotube (MWNT) and its contacts, welded to a coplanar waveguide (CPW), was measured up to 24 GHz using a technique that removes environment effects. This is the first time MWNT contact effects have been systematically isolated from the CPW. Each contact response was quite different and also showed a pronounced sensitivity to ambient light. Adding more contact material clearly changed the high-frequency electrical response and the sensitivity to light.

Carbon nanotubes are a basic building block for nanometer-scale electronic devices. Nanoelectronic structures using nanotubes include field effect transistors, field emission electron sources and connective wiring. Characterizing the electrical properties of these new electrical components is fundamental to commercializing the next generation electronics. For example, in certain configurations, one of the most dramatic and promising properties of carbon nanotubes is the very high electrical conductivity. In devices this allows for high currents with low resistive heating. This property, referred to as ballistic conduction, is due to very low scattering as the electrons pass through the nanotube. However, the contacts between nanotubes and other circuit materials can have very high and widely varying impedance, limiting the circuit improvements of which nanotubes are capable. Characterizing these contacts is a key step in enabling nanotube-based electronics by identifying not only which contacts have problems but also the nature of the electrical problem. To address this issue, we have used a combination of standard broadband electrical measurement techniques to measure the high-frequency response of nanotube test structures. This technique can be used to model the high-frequency impedance of these test structures as well as isolate and identify problems occurring at the nanotube contacts.

Single-walled nanotubes (SWNT) have the greatest potential for ultra small electronics; however, device fabrication using SWNTs is still in its infancy. Current nanotube device fabrication techniques are limited to electrophoretic deposition of nanotubes from solutions, direct growth of nanotubes on circuits, or micromanipulation of individual nanotubes in the scanning electron microscope (SEM).[1,2,3] Micromanipulation in the SEM, although not a mass production technique, is a straightforward technique available to fabricate devices and one that can be implemented in most laboratories equipped with an SEM. Unfortunately, the resolution available in the SEM and micromanipulator technology are not quite adequate to manipulate SWNTs.

For our experiments, we have chosen to work with multiwalled nanotubes (MWNT), which are concentric tubes within tubes that are not usually ballistic conductors. The multiple walls can have either metallic or semiconducting characteristics. These electrical hybrid tubes could be expected to behave as metallic nanowires due to the average current density across the characteristically different walls and also wall-to-wall conduction within the MWNT, which allows the metallic tubes to dominate transport. Correspondingly, other researchers have reported that at frequencies of several kilohertz, similar MWNTs have been shown to behave as diffusive conductors.[4,5]

To date, several investigations[6−12] have indicated the potential of individual carbon nanotubes as high-frequency interconnects and as building blocks for high-frequency devices, such as transistors.[13,14] However, broadband electri-

10.1021/nl062725s This article not subject to U.S. Copyright. Published 2007 by the American Chemical Society
Published on Web 03/22/2007

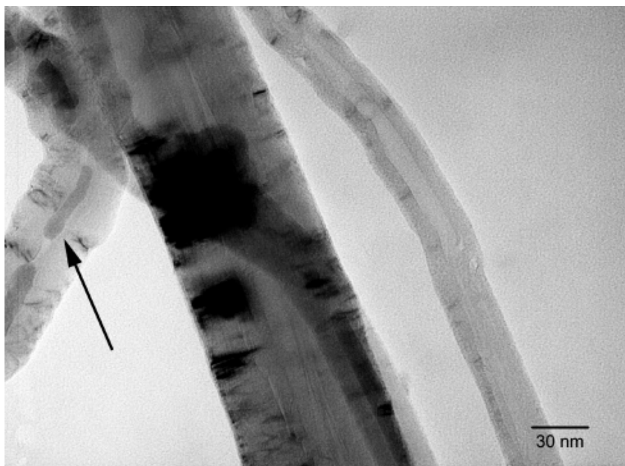

Figure 1. TEM image of typical MWNT used in these experiments. Residual catalyst can be seen inside the left nanotube as indicated by the arrow. Dark areas on the large nanotube are defects.

cal characterization of individual carbon nanotubes and other nanoscale systems is still in the early stages of development. This metrology faces a significant number of challenges, including large impedance mismatch, strong frequency dependence of the impedance, and the need to distinguish the properties of the carbon nanotubes from the test platform. Some recently reported examples of this work are as follows: Burke et al. developed high-frequency models of nanotubes and have performed a one-port measurement of a nanotube up to 10 GHz,[6−8] Yngvesson reported methods based on heterodyne mixing,[9] Zhang et al. made calibrated, two-port measurements of as few as five SWNTs in parallel up to 20 GHz,[10] and Bethoux et al. performed calibrated measurements of field effect transistors based on a random network of carbon nanotubes up to 8 GHz.[11] Several high-frequency nanotube transistors have been demonstrated.[13,14] These examples have reported excellent progress toward measuring the electrical properties of nanotubes or devices made from nanotubes. Though contact resistance is present in all of these examples and its dominant contribution to total resistance of SWNTs has been suggested by Yu and Burke,[8] the above studies have not been able to independently demonstrate the role of contacts in determining the high-frequency electrical properties of nanotubes.

To explore the electrical properties of these contacts, we have mounted individual MWNTs onto coplanar waveguides (CPW) and measured the response of the nanotubes up to 24 GHz using a technique similar to one for measuring high-frequency electrical signals with high-impedance probes.[15] The nanotubes were mounted to a thin-film microlithographically patterned Au CPW in the SEM by use of a micromanipulator. The CPW was developed for 2- and 4-port measurements. Electron beam-induced-deposition (EBID) of carbon was used to weld the nanotubes to the CPW.[16]

The nanotube used in these measurements was from a batch of MWNTs that ranged in diameter from 30 to 100 nm and in length from 5 to 40 μm. Seen in Figure 1 is a transmission electron microscope (TEM) image of a typical carbon nanotube used for these measurements. There could be up to 100 walls in these tubes, although they are not quite visible in this image. These tubes were synthesized by chemical vapor deposition (CVD) on a thin-film Fe catalyst. Precursor gases were xylene and ferrocene, and the furnace temperature during synthesis was 725 °C. The tubes were mechanically scraped from the catalyst substrate into toluene and then dried onto a glass substrate.

The nanotube was mounted to the CPW as follows: First, carbon-impregnated SEM tape was dragged across the glass substrate leaving a few nanotubes exposed horizontally on the edge of the tape. Second, the tubes and the supporting tape were placed in the SEM and the tubes were moved from the tape to the CPW with a tungsten probe mounted to a micromanipulator. Finally, the tubes were welded in place on the CPW.

To create the weld (contact) in the SEM, the electron beam is held on a spot where a connection is desired. The SEM used in these experiments was an older (1992) diffusion-pump-based microscope.[17] The electron beam has enough energy to split hydrocarbon molecules, which are common contaminants in diffusion-pump-based SEMs. The resultant active carbon condenses on the nanotube and substrate to form a strong bond or weld. It is generally assumed that this weld is comprised of amorphous carbon. The electron beam was left focused on each weld for 5−10 min with a beam current of 7 nA at 5 kV accelerating voltage. Typical SEM chamber pressure during formation of the welds was 8×10^{-4} Pa (6×10^{-6} Torr).

After the MWNT was welded to the CPW, the high-frequency electrical properties of the system were characterized using a commercial vector network analyzer (VNA). The scattering matrix elements S_{11}, S_{12}, S_{21}, and S_{22} of the two-port network were determined as function of frequency from 100 MHz to 24 GHz. The subscripts 1 and 2 in the scattering matrix elements refer to the left-hand and right-hand ports of the device, respectively. For a full discussion of two-port analysis, including scattering matrices, see ref 19. Additionally, an identical CPW without a MWNT was characterized by use of the VNA. This second set of measurements provides a high-frequency electrical characterization of the empty CPW, including the parasitic capacitance of the CPW. Both sets of measurements were calibrated with the multiline thru-reflect-line (TRL) method.[18] This calibration technique is essential to the experiments described here, as it provides a determination of the propagation constant of the CPW material. This, in turn, allows the reference planes for the calibrated measurements to be moved up to the edge of the welds of the MWNT. Thus, the electronic properties of the CPW up to the welds are removed from the measurement, providing sensitivity to the high-frequency properties of the MWNT as well as the contacts. Note that both CPWs, as well as the patterned structures required for the multiline TRL calibration, were fabricated on the same wafer.

A model was developed to separate the electrical properties of the individual welded MWNT from the electrical properties of the CPW structure to which it was welded. This model is similar to a recently reported model for the characterization of field-effect transistors based on a random network of

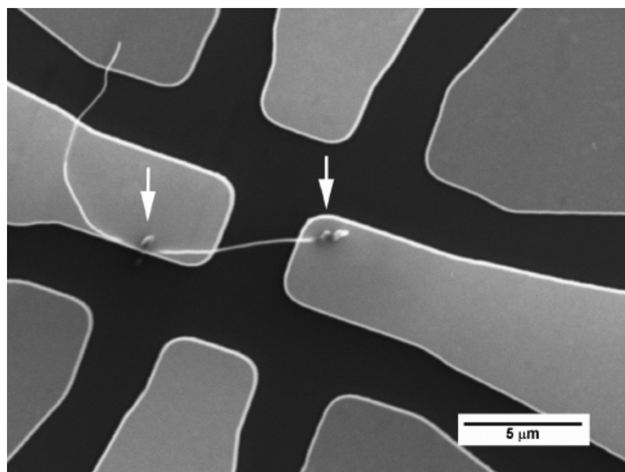

Figure 2. MWNT measured in this paper as originally welded to the CPW. The arrows indicate the contacts. The diameter of the tube is about 100 nm, and the length between the contacts is 7.5 μm. The CPW is 300 nm thick Au on a silicon substrate. Note that the MWNT is welded across two of the four electrodes available in this CPW configuration the two vertical electrodes are unused (four extensions of the ground plane are also visible in each corner of the image).

carbon nanotubes.[11] First, the measurements were converted from a scattering matrix representation to an admittance matrix representation (Y_{11}, Y_{12}, Y_{21}, Y_{22}). The subscripts 1 and 2 in the admittance matrix elements refer to the left-hand and right-hand contacts, respectively, of the nanotube to the CPW, as seen in Figure 2. The admittance matrix elements can be calculated from simple algebraic functions of the scattering matrix elements. Note that the admittance matrix elements are complex. They describe both the amplitude $|Y_{ij}|$ and phase $\arg(Y_{ij})$ of the signals reflected by and transmitted through the two-port system.[19] The admittance matrix of the total welded system ($\mathbf{Y}_{\text{total}}$) was modeled as the admittance of the MWNT, including contacts, ($\mathbf{Y}_{\text{MWNT}}$) in parallel with the admittance of the CPW gap ($\mathbf{Y}_{\text{gap}}$)

$$\mathbf{Y}_{\text{total}} = \mathbf{Y}_{\text{MWNT}} + \mathbf{Y}_{\text{gap}} \quad (1)$$

$\mathbf{Y}_{\text{total}}$ and $\mathbf{Y}_{\text{gap}}$ are known from the VNA measurements of the CPW with and without the welded MWNT, respectively. Thus, $\mathbf{Y}_{\text{MWNT}}$ can be directly calculated from the measured data using eq 1. In the remaining discussion and figure captions, Y_{11}, etc. refer to the components of the $\mathbf{Y}_{\text{MWNT}}$ matrix.

An SEM image of the MWNT as originally welded to the CPW is shown in Figure 2. Also a magnified SEM image of the original, right-hand weld is shown in Figure 3a. During the initial testing of the MWNT CPW structure, we serendipitously discovered that, as originally welded, the electronic properties showed a pronounced sensitivity to exposure to the probe station microscope light. As shown in Figure 3b, $|Y_{11}|$ and $|Y_{22}|$ changed significantly when illuminated with white light. $|Y_{11}|$ and $|Y_{22}|$ are of particular interest as they isolate the properties of the left and right-hand contacts. Note that the uncertainty in the calibrated $|S_{11}|$ and $|S_{22}|$ is about 5×10^{-3}.[20] For a high impedance load, this corresponds to

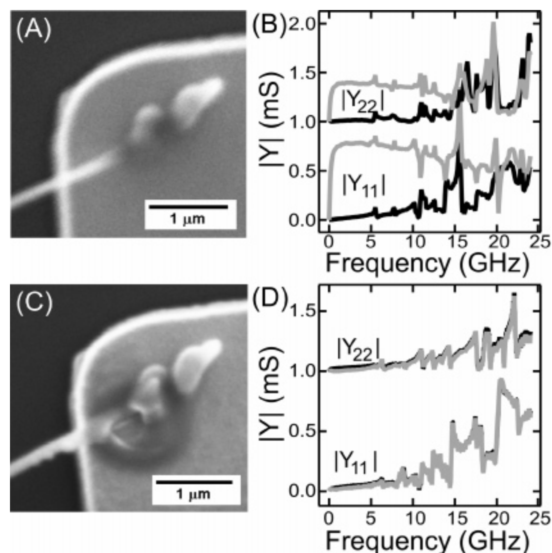

Figure 3. (a) Higher-magnification SEM image of the right contact as originally welded. (b) The electrical response of the MWNT as originally welded with the light on (gray curve) and off (black curve). (c) SEM image of right contact with more carbon added to weld. (d) The electrical response of the MWNT with the modified weld with the light on (gray curve) and light off (black curve). In (b) and (d), the $|Y_{22}|$ curves have been offset by 1 mS to facilitate comparison.

an uncertainty in $|Y_{11}|$ and $|Y_{22}|$ of about 0.1 mS. Thus, the pronounced sensitivity to light shown in Figure 3b is greater than the calibrated measurement uncertainty. More systematic studies are required to determine the precise origin of this difference in behavior with and without illumination. It is possible that this difference arises from thermal expansion of the contact when illuminated or changes in photocarrier generation within the contact or the MWNT. Note that our model should eliminate any effects that occur in both the total welded system and the identical CPW without the MWNT, such as generation of photocarriers in the Si substrate. There are several sharp resonances in the amplitudes and phases of Y_{11} and Y_{22} between 5 and 24 GHz. These are measurement artifacts that are repeatable and arise from signal coupling between the unused electrodes of the CPW structure and not from the MWNT plus contacts. The contact was then modified by repeating the welding process described above on both contacts, leading to additional deposition of carbon in the contacts. The modified right-hand weld is shown in Figure 3c. The high-frequency electrical properties of the welded MWNT clearly changed due to the modification of the contacts. As shown in Figure 3d, $|Y_{11}|$ and $|Y_{22}|$ in the modified MWNT CPW structure display little or no dependence on the exposure to white light.

However, the phases $\arg(Y_{11})$ and $\arg(Y_{22})$ in the modified MWNT CPW structure are dissimilar. As shown in Figure 4b, $\arg(Y_{11})$ tends to increase with frequency, whereas $\arg(Y_{22})$ tends to decrease with frequency. This difference in phase is attributed to the presence of a tail at the end of the MWNT to the left of the left-hand contact, as seen in Figure 2. The presence of the tail changes the impedance of the contacts and the load. The MWNT tail was then removed with the micromanipulator, as shown in Figure 4a. With the

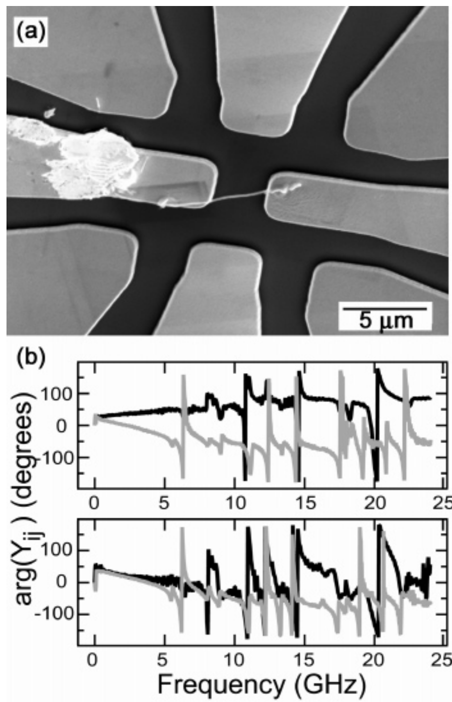

Figure 4. (a) SEM image of the structure after nanotube tail was removed. (b) The frequency response of the phases arg(Y_{11}) (black curves) and arg(Y_{22}) (gray curves) measured before (top set of data) and after (bottom set of data) tail was removed.

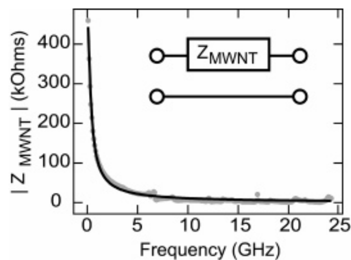

Figure 5. Amplitude of the MWNT impedance is shown as a function of frequency. The gray circles indicate the measured data. The black line indicates a fit to the data, assuming a resistor ($R = 0.47$ MΩ) in parallel with a capacitance ($C = 1.4$ fF). The assumed circuit model is shown in the inset.

tail removed from the structure, arg(Y_{11}) and arg(Y_{22}) display the same trend with frequency. Note that there are still some significant differences between arg(Y_{11}) and arg(Y_{22}) over certain frequency ranges that are attributable to differences in the positions of the contacts on the metallic pads and structural differences in the patterned CPW.

Finally, we note that the measurements and model presented here may be used to determine the impedance of the welded MWNT. $\mathbf{Y}_{MWNT}$ can be converted to $\mathbf{Z}_{MWNT}$. As a first approach, we assume that the equivalent circuit model of $\mathbf{Z}_{MWNT}$ is as shown in Figure 5, inset. We have chosen this simple model for a first order analysis of the data, but this model is not the only model that is consistent with the data. This simplified model is a first approach and a full $\mathbf{Z}_{MWNT}$ impedance matrix may be calculated via more rigorous modeling. The frequency dependence of $|Z_{MWNT}|$ from 100 MHz to 24 GHz is shown in Figure 5. $|Z_{MWNT}|$ varies widely, from 150 to 175 kΩ at low frequencies to about 1 kΩ near 24 GHz. This is consistent with theoretically predicted values[21] and can be understood in a straightforward way. If we assume that the modeled impedance $\mathbf{Z}_{MWNT}$ consists of a resistance R in parallel with a capacitance C, then the corresponding fit to the data in Figure 5 produces $R = 0.47$ MΩ and $C = 1.4$ fF. We choose a parallel rather than series configuration of R and C as it fits the frequency dependence of the extracted data. We stress that this is a simplified model, and a more complex circuit is required for a complete physical model.

In summary, we were able to measure the admittance/impedance of a MWNT with EBID formed contacts to a microlithographic CPW test structure at frequencies up to 24 GHz. We have shown that with precise TRL calibrations broadband 2-port measurements are a sensitive method to characterize nanoscale contacts, geometries, and circuit parameters. We have identified several interesting high-frequency electrical phenomena for this test structure. The electrical properties of the contacts are very dependent on the geometry of the contact and also the EBID process. First, when we removed the superfluous nanotube from outside of the active area on the structure, we see an improvement in the electrical response, which we gauged from the similarity of the phase of the electrical response of the two contacts. Second, we observed that the contact's electrical response is sensitive to ambient light. Although we do not yet know the mechanism for this sensitivity, when we increase the quantity of the EBID carbon coating on the contact, we see improvement in the electrical response. Both of these observations of the contacts indicate issues that will need to be addressed in the future for carbon nanotube based electronics.

Acknowledgment. We thank Professor E. Gruelky for the MWNTs.

References

(1) Javey, A.; Guo, J.; Wang, Q.; Lundstrom, M.; Dai, H. *Nature* **2003**, *424*, 654.
(2) Huang, X. M. H.; Caldwell, R.; Huang, L.; Jun, S. C.; Huang, M.; Sfeir, M. Y.; O'Brien, S. P.; Hone, J. *Nano Lett.* **2005**, *5*, 7.
(3) Lu, S.; Chung, J.; Ruoff, R. S. *Nanotechnology* **2005**, *16*, 1765.
(4) Schönenberger, C.; Bachtold, A.; Strunk, C.; Salvetat, J.-P.; Forró, L. *Appl. Phys. A* **1999**, *69*, 283.
(5) Bachtold, A.; Fuhrer, M. S.; Plyasunov, S.; Forero, M.; Anderson, E. H.; Zettl, A.; McEuen, P. L. *Phys. Rev. Lett*. **2000**, *84*, 6082.
(6) Burke, P. J. *IEEE Trans. Nanotechnol.* **2003**, *2*, 55.
(7) Li, S. D.; Yu, Z.; Yen, S. F.; Tang, W. C.; Burke, P. J. *Nano Lett.* **2004**, *4*, 753.
(8) Yu, Z.; Burke, P. J. *Nano Lett.* **2005**, *5*, 1403.
(9) Yngvesson, K. S. *Appl. Phys. Lett.* **2005**, *87*, 043503.
(10) Zhang, M.; Huo, X.; Chan, P. C. H.; Liang, Q.; Tang, Z. K. *Appl. Phys. Lett.* **2006**, *88*, 163109.
(11) Bethoux, J.-M.; Happy, H.; Dambrine, G.; Derycke, V.; Goffman, M.; Bourgoin, J.-P. *IEEE Electron Device Lett.* **2006**, *8*, 681.
(12) Naeemi, A.; Meindl, J. D. *IEEE Electron Device Lett.* **2006**, *27*, 338.
(13) Rosenblatt, S.; Lin, H.; Sazonova, V.; Tiwari, S.; McEuen, P. L. *Appl. Phys. Lett.*, **2005**, *87*, 153111.
(14) Pesetski, A. A.; Baumgardner, J. E.; Folk, E.; Przybysz, J. X.; Adam, J. D.; Zhang, H. *Appl. Phys. Lett.* **2006**, *88*, 113103.
(15) Kabos, P.; Reader, H. C.; Arz, U.; Williams, D. F. *IEEE Trans. Microwave Theory Tech.* **2003**, *51*, 530.
(16) Ding, W.; Dikin, D. A.; Chen, X.; Piner, R. D.; Ruoff, R. S.; Zussman, E.; Wang, X.; Li, X. *J. Appl. Phys*. **2005**, *98*, 014905.

(17) JEOL JSM 6100 scanning electron microscope, Such identification is not intended to imply recommendation or endorsement by NIST, nor is the equipment identified necessarily the best available for the purpose.
(18) Marks, R. B. *IEEE Trans. Microwave Theory Tech.* **1991**, *39*, 1205.
(19) Pozar, D. M. *Microwave Engineering*; Addison-Wesley: Reading, MA, 1993; p 205.
(20) Williams, D. F.; Wang, C. M.; Arz, U. *2003 International Microwave Symposium Digest*; NIST: Boulder, CO, 2003; p 1819; http://boulder.nist.gov/div818/81801/dylan/papers/MultilineNoise.pdf.
(21) Saluhuddin, S.; Ludstrom, M.; Datta, S. *IEEE Trans. Electron Devices* **2005**, *52*, 1734.

NL062725S